Theory of Burst-Mode Receiver and Its Applications in Optical Multiaccess Networks

Chao Su, Lian-Kuan Chen, and Kwok-Wai Cheung, *Senior Member, IEEE*

***Abstract*—In this paper, a unified theory for the newly developed optical burst-mode receiver is presented. Based on this theory, an analysis of the performance of the receiver is given both theoretically and experimentally. The theoretical model agrees well with the experimental results. This theory can quantitatively explain the bit error rate (BER) performance of burst-mode receivers. Several potential applications of burst-mode receivers are also illustrated, including applications in supervisory system for erbium-doped fiber amplifier (EDFA) trans-oceanic optical links and various high-speed all-optical multiaccess packet networks.**

I. Introduction

THE next-generation optical networks will likely require fast packet switching (e.g., ATM) to support multimedia applications, and an ultrahigh transmission speed is very desirable. As the bit rate increases to beyond what electronic processing can comfortably handle, it is increasingly desirable to reduce the amount of regenerative electronic processing at each node. Recent advances in fiber-optic technology (e.g., erbium-doped fiber amplifier (EDFA), high-speed time multiplexing/demultiplexing, high density wavelength division multiplexing (WDM) devices, optical tunable filter, etc.) have prompted researchers to envision a future all-optical network that is capable of supporting multiple access and services at very high bit rate.

In these all-optical multiaccess networks, any node can use a designated time slot to send a packet to some other nodes. A very significant feature of these all-optical multiaccess network which is different from conventional point-to-point links is that the amplitude and phase of the received packets can be quite different from packet to packet due to different fiber attenuation and the chromatic dispersion caused by the variation of the transmitters' wavelengths. The amount of amplitude and phase variations between two bursty data packets can be up to 20 dB and 360°.

Conventional receivers are not suitable for burst-mode operation because they cannot instantaneously handle the different arriving packets with large difference in optical power and phase alignment. It is therefore necessary to design receivers which can adapt to the variation in optical power and phase alignment on a packet-by-packet basis. These types of receivers are called burst-mode receivers.

The burst-mode receiver was first realized by Ota and Swartz [1], [2] for high-speed optical data transmission systems. By using a few preamble bits in the data stream to determine the detection threshold for the subsequent burst, a dc-coupled burst-mode optical receiver with an automatic threshold control circuit was realized [2]. The receiver sensitivity was -37.5 dBm [bit error rate (BER) $<10^{-9}$] at a bit-rate of 900 Mb/s with a dynamic range of 23 dB. In [3], a novel high speed PIN HBT monolithic photoreceiver was demonstrated for both continuous and burst-mode format. The measured sensitivities were -21.5 and -18.6 dBm at 2.5 and 5 Gb/s, respectively, under continuous mode operation. A power penalty of 1.5 dB for burst-mode operation was also observed but unexplained.

There are two intrinsic effects that degrade the BER performance of burst-mode receivers. First is the random Gaussian noise which is always present at the receiver that affects the determination of the decision threshold and introduces sensitivity penalty. This problem was first addressed by Eldering [4] who computed the BER penalty due to Gaussian noise during the determination of threshold setting from the preamble field. A more accurate theoretical model was provided in [5]. The second effect comes from the finite charging/discharging time of the adaptive threshold detection circuitry in the receiver [6]. We provide a unified framework in this paper to study the interaction of these two effects. The result shows that the BER penalty is relatively independent of the length of the preamble field when the discharging time is finite. This contrasts quite sharply with the result in [4] when the discharging time is infinite.

Burst-mode receivers are very suitable for many high-speed optical multiaccess network applications using regenerative or nonregenerative packet transmissions. For example, the receivers can be employed in passive optical networks [(PON) tree topology using time division multiple access (TDMA)], optical bus networks, WDMA optical star network, multichannel parallel optical data link, supervisory system for undersea/long-hauled EDFA transmission systems, etc. For all these applications, the requirements for the burst-mode receivers are as follows:

Manuscript received August 14, 1995; revised August 15, 1996. This work was supported by the University Grant Committee of Hong Kong under RGC Grant CUHK499/95E. The work of C. Su was supported by a Postdoctoral Fellowship from the Chinese University of Hong Kong.

C. Su was with the Department of Information Engineering, The Chinese University of Hong Kong, Shatin, N.T., Hong Kong. He is now with QPS Technology Inc., Dorval, P.Q., Canada.

L.-K. Chen and K.-W. Cheung are with the Department of Information Engineering, The Chinese University of Hong Kong, Shatin, N.T., Hong Kong.

Publisher Item Identifier S 0733-8724(97)02687-X.

1) large dynamic range to allow network flexibility;
2) fast response time to improve detection of short packet or burst data;
3) simplicity and robustness to improve network reliability.

This paper is divided into two parts. In the first part, we present a unified framework to explain the BER performance of various kinds of burst-mode receivers. The results are compared both analytically and experimentally. The theory provides a better understanding of the BER performance of the burst-mode receivers and explains the origin of the BER penalty. It also provides insight to the design of burst-mode receivers which may open up new possibilities for the future generations of burst-mode receivers.

In the second part, we suggest several applications of burst-mode receivers in optical multiaccess packet networks. First is the application in supervisory system for EDFA trans-oceanic optical links. Second, we discuss the role of burst-mode receivers in high-speed all-optical multiaccess packet networks with different topologies, thus showing that burst-mode receivers are very suitable for all these types of all-optical multiaccess packet networks.

II. Theory of Burst-Mode Receivers

A. Conventional Versus Burst-Mode Receivers

In this section, we shall present a theory for burst-mode receivers. First, we clarify what the burst-mode data is, and illustrate the differences between the conventional receiver and the burst-mode receiver.

Generally speaking, there are three types of signal format in digital communication systems as shown in Fig. 1. Fig. 1(a) Pattern 1 is known as the continuous mode data. A binary sequence is continuously sent with an approximately balanced ratio of 1's to 0's, and the interval between any two logic transitions is strictly limited. Examples are the 4B5B or mBnB line codes commonly used in point-to-point data link applications. Fig. 1(b) Pattern 2 is known as the burst-mode data, where the ratio of 1's to 0's and the intervals between the logic transitions are not constrained. The sequences have the same amplitude for the same logic symbols. A good example is the point-to-point low speed data link for computers using the RS-232 interface.

For Fig. 1(c) Pattern 3, the signal amplitude may vary from packet to packet, and a guard time is usually used between different packets. These kinds of patterns usually appear in the packet transmission of multiaccess networks such as the Ethernet. The data format is referred to as the burst and packet mode data in the literature [7]. We shall call these patterns "packet data" for simplicity. The task for a burst-mode receiver is to recover Patterns 2 or 3 correctly and instantaneously.

In a conventional receiver, ac coupling is used. The ac-coupled circuitry can provide high sensitivity for the receiver. However, because of the charging and discharging time of the capacitors associated with the ac-coupled signal path, the average amplitude of the received data is not allowed to vary rapidly with time. Therefore, conventional receivers are only suitable for continuous mode data reception.

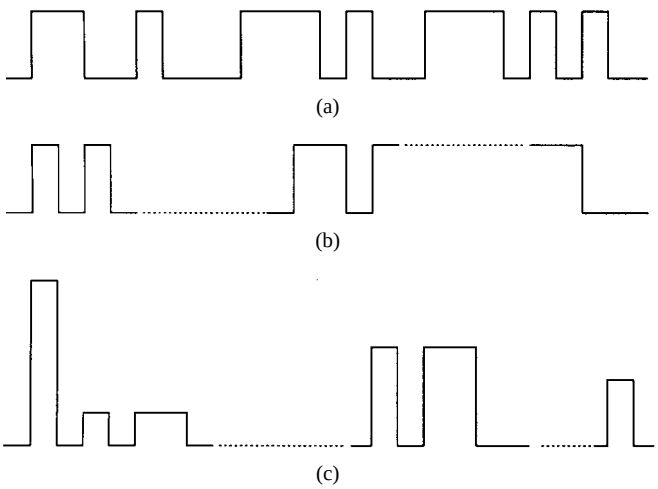

Fig. 1. An example for three data formats in digital communication. (a) Pattern 1: Continuous mode data. (b) Pattern 2: Burst-mode data. (c) Pattern 3: Burst and packet mode data.

TABLE I
Comparison of Conventional and Burst-Mode Receiver

Receiver	Conventional	Burst-Mode
Signal Coupling	ac	dc
Threshold Setting	Fixed	Adaptive
Amplitude and Clock Recovery Time	μs	ns
Access Time for Receiver	μs	ns

The operation of a burst-mode receiver is very different from a conventional receiver. The main difference is that the burst-mode receiver is dc-coupled and the threshold setting of the receiver circuitry must adapt to the amplitude of received signal in a very short time. Second, clock and phase recovery of a burst-mode receiver must be performed very quickly (typically within a small fraction of a packet transmission time). Table I summarizes the differences between the two types of receivers.

B. Different Types of Burst-Mode Receivers

Burst-mode receivers can be divided into two types according to their structures: 1) feedback type [1] and 2) feedforward type [4]. Examples of these two types are shown in Fig. 2. Type 1 uses a differential input/output trans-impedance amplifier with a peak detection circuit forming a feedback loop. The peak detector circuit determines the instantaneous detection threshold for the incoming signal. The output of the preamplifier is dc-coupled to a differential postamplifier for further amplification. In this scheme, the signal's amplitude recovery is done in the pre-amplifier.

In type 2 receivers, a conventional dc-coupled pre-amplifier can be used. The received signal is first amplified by this preamplifier and then split into two branches. The first branch of the output from the pre-amplifier is dc-coupled to a differential amplifier. The second branch is feedforward into a peak detection circuitry to extract the amplitude information of received packets. From the output of the peak detector, the proper threshold level can be set adaptively in front of the differential amplifier. At the output of the differential

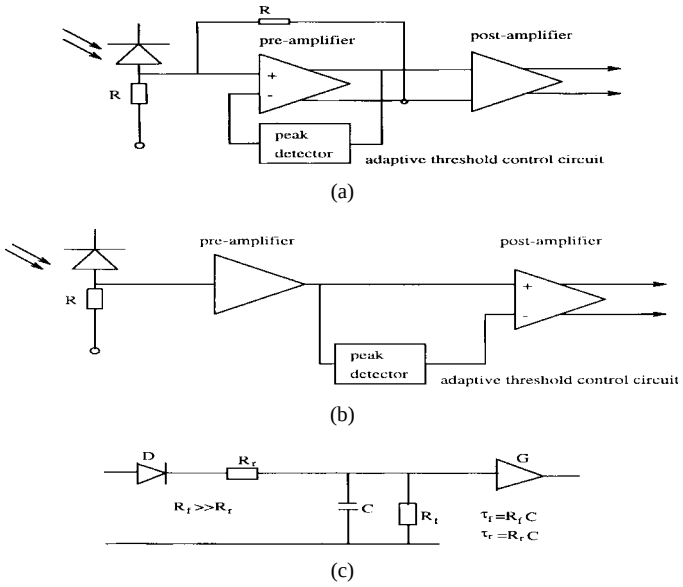

Fig. 2. Two types for the operation of optical burst-mode receiver. (a) A feedback type burst-mode receiver. (b) A feedforward type burst-mode receiver. (c) A peak detection circuitry.

amplifier, the amplitude-recovered data packet is ready for further processing.

It should be noted that the analysis presented in this paper is independent of the burst-mode receiver's configurations, i.e., both types 1 and 2 are applicable. As far as the hardware implementation is concerned, the operation for type 1 is more stable than type 2, since a feedback loop enables the receiver to work more reliably, but a differential input/output preamplifier is needed. In type 2, a conventional dc-coupled preamplifier can be used in the receiver, however, the circuitry needs to be carefully designed to prevent oscillation in the receiver.

In the literature, burst-mode receivers have also been classified according to the way the threshold is set. The first type is that the receiver threshold is determined completely from the preamble field and held constant in the data field [4], [5]. The second type is that the receiver threshold is adaptively determined according to the input signal [1]–[3].

In this paper, we provide a unified framework for characterizing the BER performance of all burst-mode receivers using only two parameters, namely, the rise time constant and the holding time constant of the adaptive threshold detection circuit. The first type above [4], [5] has a finite rise time constant and an infinite holding time constant whereas the second type above [1]–[3] has a small rise time constant but a finite holding time constant. Both types can be regarded as special cases in our unified framework.

C. Amplitude Recovery

In general, the BER performance of burst-mode receivers is affected by both the adaptive threshold control circuit and the clock recovery circuit. First we discuss the effect of the adaptive threshold control circuit on the amplitude recovery process.

It is well known that for a conventional receiver, the BER is

$$P_e = P(0)P(1|0) + P(1)P(0|1) \tag{1}$$

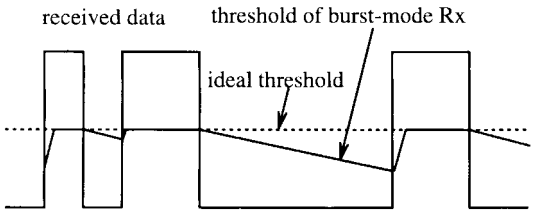

Fig. 3. The threshold variation of a burst-mode receiver.

where $P(0)$ and $P(1)$ are the probability of logic 0 and 1, respectively, $P(1|0)$ is the probability of 1 when a 0 is transmitted and $P(0|1)$ is the probability of 0 when a 1 is transmitted. Both $P(0|1)$ and $P(1|0)$ depend on the setting of the amplitude threshold, which is usually set to a fixed optimal level according to the steady state signal amplitude and noise statistics (see, e.g., [8]). The steady-state amplitude threshold is determined by integrating the signal over a long period of time.

In a multiaccess network employing burst-mode receivers, the BER performance of the receiver should approach that of a conventional receiver after the connection between two nodes (via packets) has settled into steady state. However, because of noise in the receiver and the finite rising/holding time constant of the adaptive threshold control circuit, the detected threshold level is not constant but fluctuates around the ideal threshold according to the incoming data pattern (shown in Fig. 3), thus causing a degradation in the BER performance.

Because the receiver performance depends on its threshold detection, to distinguish it from the conventional receiver's BER, we define the BER of a burst-mode receiver as

$$P_e = P(0)P_{e0} + P(1)P_{e1} \tag{2}$$

where $P(0)$, $P(1)$ are the probabilities of 0's and 1's appearing in the data Pattern, P_{e0} and P_{e1} are the error probabilities caused by 1's and 0's in the burst-mode receiver.

1) Extraction of Threshold from the Preamble Field: The major difference between burst-mode and conventional receiver is that the threshold detection in burst-mode receiver must adapt to the incoming signal in a very short time frame, thus the threshold is susceptible to corruption by noise. Assume that the received signal is corrupted by additive white Gaussian noise (AWGN). The instantaneous threshold determined by the adaptive threshold detection circuit (represented by the random variable r) has a Gaussian distribution. We call this variable the noise corrupted threshold (NCT). If l preamble bits are used to determine the threshold, the probability density function for NCT r is [4]

$$f(r) = \frac{1}{\sigma}\sqrt{\frac{l}{2\pi}}\,\exp\left[\frac{-l(r - V_{th}^{l})^2}{2\sigma^2}\right] \tag{3}$$

where V_{th}^{l} is the mean value of the NCT determined from the l preamble bits, and σ is the rms noise averaged over one bit.

Reference [4] provided a model to evaluate the receiver's BER performance using only the preamble bits for the detection of the threshold. It has been suggested that by properly choosing the rising time constant of the peak detector, it

is possible to make the charging time correspond to the l-bits of the preamble. From the computation, it is shown that when one, four, and eight bits are used for the threshold determination, the resulting SNR (electrical) penalty are 3, 0.94, and 0.5 dB, respectively, relative to the conventional receivers. Obviously, the receiver will have a better performance with a large rising time constant and a large number of preamble bits which averaged out the Gaussian white noise. Using a weighting factor, [5] provided a more complete model for the noise corrupted amplitude recovery by means of an integrative detector and extended the analysis to signal-dependent Gaussian noise and threshold detection by a peak detector. The result shows that the distribution of the detected threshold is an asymmetric function. Both of these models are applicable to the evaluation of the receiver's performance where the threshold is determined entirely from the preamble field.

In many applications, the preamble data format is not all 1's but chosen to be like "101 010$\cdots$" (e.g., Ethernet) for the convenience of amplitude and clock recovery of the transmitted packet in the network. Since the holding time constant of the peak detector is usually very large and the threshold decay is small, the models provided by [4], [5] are still valid in these cases.

2) Rising and Holding Time Constant Consideration: There are other kinds of burst-mode receivers [1]–[3] where the detection threshold is adaptively changed according to the incoming signal. In this section, we consider the effect of the rising and holding time constant of the peak detector on the threshold setting. An expression will be derived for the instantaneous and bit-average threshold as a function of the rising time and holding time constants.

For these burst-mode receivers using adaptive threshold determination (Fig. 3), the detected threshold in the data field can be represented by a Markov process

$$V_{th}[m,\,t] = \begin{cases} V_{th}[m-1,\,T]\exp(-t/\tau_f) & a(m)=0 \\ V_{th}[m-1,\,T] + (V_c - V_{th} \\ \quad \times[m-1,\,T])[1-\exp(-t/\tau_r)] & a(m)=1 \end{cases} \tag{4}$$

where $V_{th}[m,\,t]$ is the threshold at time t in the mth bit-interval, t is measured with respect to the start of each bit-interval, i.e., $0 \le t \le T$, T is the bit-interval, $a(m)$ is the data symbol ("0" or "1") for the mth bit, V_c is the optimal threshold if the signal is received by a conventional receiver, and τ_r and τ_f are the rising and holding time constant for the peak detection circuitry as shown in Fig. 2. We have taken the "0" level to be zero for simplicity.

In Fig. 2, we define the rising parameter K_r and decay parameter K for the peak detection circuitry as

$$K_r = \frac{T}{\tau_r}$$
$$K = \frac{T}{\tau_f}. \tag{5}$$

Here, we compute the average threshold for the mth bit of the packet (averaged over the entire bit). Assuming the data symbol to be 1, it can be expressed as

$$\begin{aligned} \overline{V}_{th1} &= \frac{1}{T}\int_0^T V_{th}[m,\,t]dt \\ &= V_c - V_c(1-\alpha)\frac{1-e^{-K_r}}{K_r} \end{aligned} \tag{6}$$

where $\alpha = V_{th}[m-1,\,T]/V_c$, and $V_{th}[m-1,\,T]$ is the threshold of the previous bit. It should be noted that α depends on the input data pattern.

If the data symbol is 0, the instantaneous threshold of the bit under consideration depends on the number of consecutive 0's in the input data preceding the bit, because the threshold will decay from the initial value $V(0)$ to a smaller value. Thus, the signal-to-noise ratio (SNR) of the receiver is reduced [6] and a power penalty is introduced.

Assume a long string of consecutive 0's appear in the input signal. The average threshold V_{th} for the jth consecutive 0 bit is given by

$$\begin{aligned} \overline{V}^j_{th0} &= \frac{1}{T}\int_{(j-1)T}^{jT} V_{th}[j,\,t]dt \\ &= \frac{e^{-(j-1)K} - e^{-jK}}{K} \times V(0) \end{aligned} \tag{7}$$

where $V(0)$ is the initial value of the threshold before the start of the string of consecutive 0's

$$V(0) = V_c - V_c(1-\alpha)e^{-K_r}. \tag{8}$$

Suppose the initial threshold is zero at the beginning of a data packet. After l-bits of consecutive 1's, the threshold is

$$V^l_{th} = V_c(1-e^{-lK_r}). \tag{9}$$

Since V^l_{th} can only approach V_c when lK_r is large where l is the number of consecutive 1 bits, we can define a steady-state error ϵ as

$$\epsilon = \frac{V_c - V^l_{th}}{V_c}. \tag{10}$$

Thus, we have the following relationship:

$$\begin{aligned} K_r &= -\frac{\ln\epsilon}{l} \\ V^l_{th} &= V_c(1-\epsilon). \end{aligned} \tag{11}$$

Here, ϵ is taken to be 2% in order to provide a conversion formula between K_r and l for our subsequent analysis. From the above equations, we can evaluate the BER performance of the burst-mode receiver in the next section.

D. A Unified Model for Burst-Mode Receivers

Here we present a unified model for analyzing the BER performance of burst-mode receivers. We consider two types of binary baseband data: encoded data (mBnB line coded) and uncoded data (pseudo-random signal). For encoded data, the binary sequence has an approximately balanced ratio of 1's to 0's, and the maximum length of consecutive symbols is strictly limited. For the uncoded data, the maximum

TABLE II
THE DISTRIBUTION OF CONSECUTIVE 0'S IN ENCODED 4B5B AND 5B6B DATA

0's in Data	4B5B Code	5B6B Code
$P_1(0)$	0.21	0.18
$P_2(00)$	0.079	0.071
$P_3(000)$	0.008	0.02

length is determined by the generator of the pseudo-random signal.

For a pseudo-random input signal of length $N = 2^n - 1$ where N is the length of the pseudorandom number sequence (PRNS), the ratio of 0-bits contained in strings of i-consecutive 0's relative to N is $1/2^{i+1}$. After some algebraic manipulations, the average BER can be expressed as

$$\begin{aligned} P_e &= P(1)\overline{P}_{e1} + P(0)\overline{P}_{e0} \\ &= P(1)\int_{-\infty}^{+\infty} f(r)P_{e1}\,dr \\ &\quad + \sum_{i=1}^{n}\frac{1}{2^{i+1}}\,\frac{1}{i}\sum_{j=1}^{i}\int_{-\infty}^{+\infty} f(r)P_{e0j}\,dr \\ &= \frac{1}{2}\,\mathrm{BER}\,(1) + \sum_{i=1}^{n}\frac{1}{2^{i+1}}\,\frac{1}{i}\sum_{j=1}^{i}\mathrm{BER}^j(0) \end{aligned} \tag{12}$$

where

$$\begin{aligned} \mathrm{BER}(1) &= \sum_{k=1}^{n} P_k \int_{-\infty}^{+\infty}\frac{\sqrt{l}}{2\pi} \\ &\quad \times \exp\left\{-\frac{l}{2}\left[Q_c(1-\alpha)\,\frac{1-e^{-K_r}}{K_r} - x\right]^2\right\} \\ &\quad \times \frac{\exp\dfrac{-(Q_c+x)^2}{2}}{Q_c+x}\,dx \\ \mathrm{BER}^j(0) &= \sum_{k=1}^{n} P_k \int_{-\infty}^{+\infty}\frac{\sqrt{l}}{2\pi} \\ &\quad \times \exp\left[-\frac{l}{2}\left(Q_c\left\{1-[1-(1-\alpha)e^{-K_r}]\right.\right.\right. \\ &\qquad \left.\left.\left. \times\frac{e^{-(j-1)K}-e^{jK}}{K}\right\} - x\right)^2\right] \\ &\quad \times \frac{\exp\dfrac{-(Q_c-x)^2}{2}}{Q_c-x}\,dx \end{aligned} \tag{13}$$

where Q_c is the optimal SNR for a conventional receiver, $x = (V_c - r)/\sigma$, $\alpha = e^{-kK}$ is dependent on the input data pattern and P_k is the probability for k consecutive 0's in the data stream.

For encoded data, two commonly used line codes—4B5B and 5B6B data format are used for analysis. For a typical 4B5B or 5B6B encoded data format (such as that provided by Am 7968 IC from AMD), statistical distributions for consecutive 0's are obtained by simulation and results are shown in Table II.

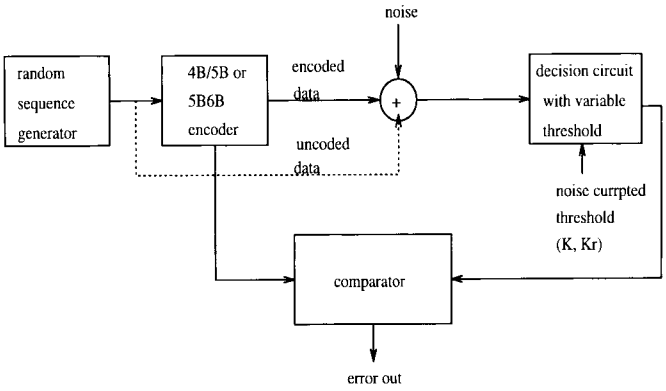

Fig. 4. A simulation diagram of BER performance for burst-mode receivers.

The BER for encoded data is

$$\begin{aligned} P_e &= P(1)\,\mathrm{BER}\,(1) + P_1\,\mathrm{BER}^1\,(0) \\ &\quad + \frac{P_2\sum_{i=1}^{2}\mathrm{BER}^i\,(0)}{2} \\ &\quad + \frac{P_3\sum_{i=1}^{3}\mathrm{BER}^i\,(0)}{3}. \end{aligned} \tag{14}$$

If we assume that $K = 0$ for the receiver, the BER performance is independent of input data format. In this case, our model converges to that in [4] and it can be expressed as

$$\begin{aligned} P_e = \int_{-\infty}^{+\infty}\frac{\sqrt{l}}{4\pi}\,\exp\left[-\frac{l}{2}\,(\epsilon Q_c - x)^2\right] \\ \times\left\{\frac{\exp\dfrac{-(Q_c+x)^2}{2}}{Q_c+x} + \frac{\exp\dfrac{-(Q_c-x)^2}{2}}{Q_c-x}\right\}dx. \end{aligned} \tag{15}$$

E. Error Performance of Burst-Mode Receiver

In order to verify our theoretical model presented above, computer simulation of the receiver performance has been performed. The simulation is shown schematically in Fig. 4. A uniformly distributed PRNS is first generated, then it goes into a transmission channel either directly (for uncoded data) or through a 4B5B/5B6B encoder (for encoded data). Gaussian noise is then added and detected by the receiver. From the received burst-mode signal's waveform, we can use (3) and the Markov relation of (4) to determine the noise corrupted threshold. We then determine the bit value of the noise-added PRNS at each sampling interval. By comparing the output sequence with the original input, we can easily obtain the BER of the receiver. By changing the value of K or K_r of the peak detection circuitry, the BER's of the receiver with respect to different K and K_r (or preamble bits) can be obtained.

In the simulation, we first evaluate the receiver BER performance due to various K. K_r is set to 0.978. This value of K_r corresponds to using four preamble bits to set the

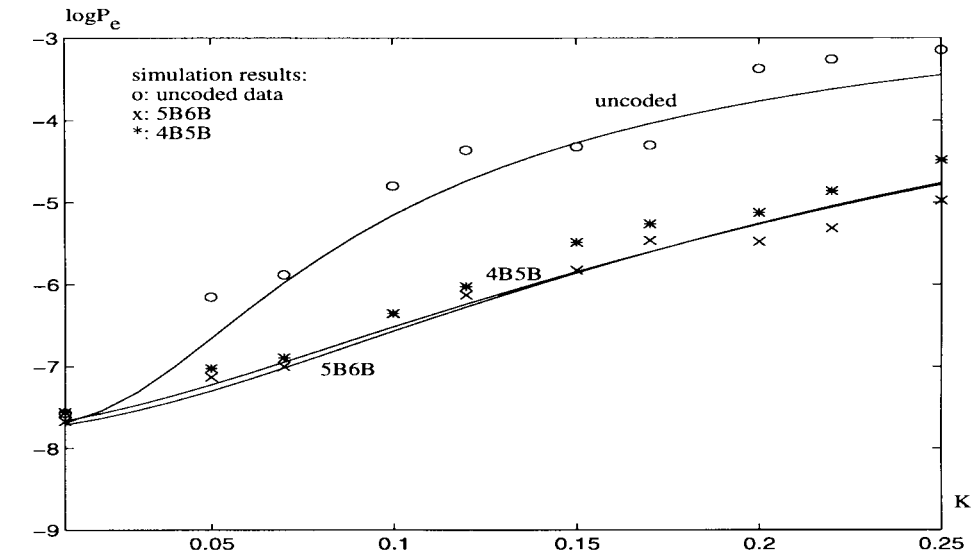

Fig. 5. BER of uncoded and encoded data versus the decay parameter K when $K_r = 0.98$. Simulation and theoretical results are shown in discrete dots and solid line, respectively, when $Q_c = 6$.

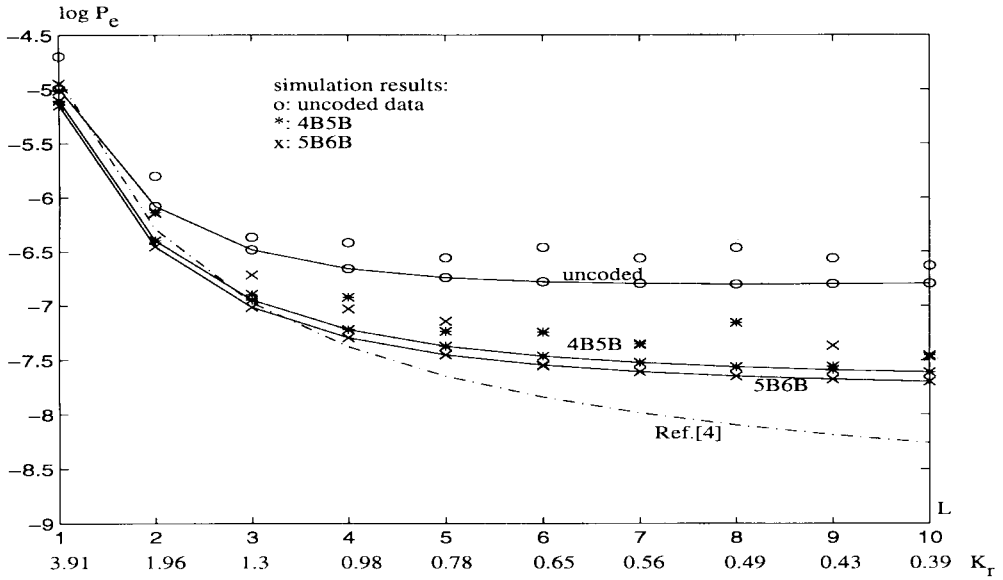

Fig. 6. BER versus K_r (or L-bits of preamble) when $K = 0.05$ and $Q_c = 6$. Simulation and theoretical results are shown in discrete dots and solid line, respectively.

threshold provided K is set to zero. The result (K versus P_e) is shown in Fig. 5. Here we compare the simulation results with the theoretical results for different data formats under the same SNR $Q_c = 6$ (which corresponds to a BER of 10^{-9} for conventional receivers). The theoretical curves agree well with the simulation results. The result shows that a large K degrades the BER performance seriously. This effect is more significant for uncoded data. This result has been reported in [6].

Next, we examine the receiver BER versus different K_r when $K = 0.05$. In Fig. 6, we show the simulation and theoretical results of P_e versus K_r for uncoded and encoded data. For comparison, the BER from [4] is also shown in the figure. It is seen that the decay effect (due to the K parameter) has considerable effect on the BER performance, and a longer preamble does not necessarily provide any significant BER improvement over four or five preamble bits.

After verifying the correctness of the equations shown in (12) and (14), we can use these equations to evaluate the receiver SNR (electrical) penalty for various K and different K_r. To facilitate a comparison with the result in [4], K_r has been chosen with values which corresponds to 1, 2, 4, and 8 preamble bits. However, we must warn that such comparison is valid only when K is zero. The model proposed here is more general than that in [4] and covers the situations when K is not zero.

The SNR penalty is plotted against the decay parameter K at BER of 10^{-9} for uncoded NRZ and 4B5B/5B6B encoded data in Figs. 7 and 8, respectively. Here, we assume that the random length of uncoded data is $N = 2^9 - 1$.

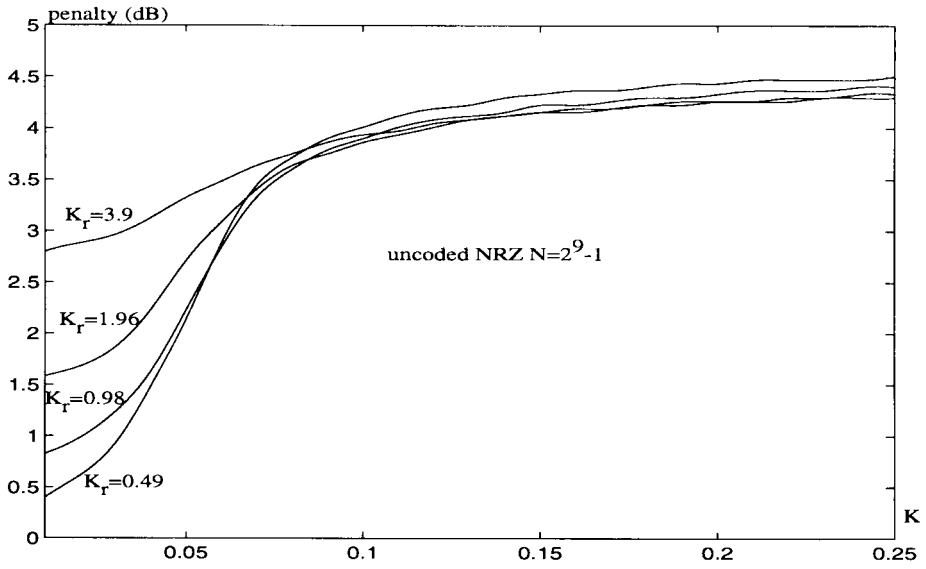

Fig. 7. SNR penalty of uncoded NRZ data versus decay parameter K for different K_r.

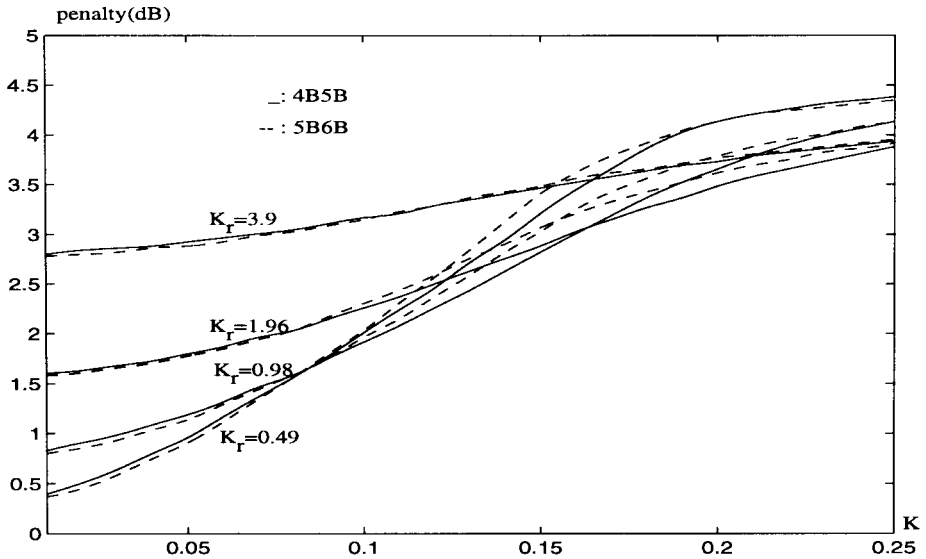

Fig. 8. SNR penalty of 4B5B/5B6B encoded data versus decay parameter K for different K_r.

In Fig. 7, it is seen that when $K \geq 0.1$, the SNR penalty is almost independent of the number of preamble bits. When $K \leq 0.1$, the receiver performance depends on both K and the length of preamble. The explanation is that when K is large, the receiver performance is dominated by the decay process of the instantaneous threshold. Similar result can be seen from Fig. 8 for 4B5B and 5B6B encoded data under different K, though the K value where the plateau occurs is much higher than the uncoded case due to the much shorter length of consecutive "0"'s.

The receiver's SNR penalty versus K_r (or preamble bits) for different K are shown in Figs. 9 and 10. For a small K (e.g., $K = 0.01$ for uncoded data), our model will converge to [4]. However, there is large difference when K is large. This is because the receiver performance due to the decay effect has not considered in [4]. From these results, it can be concluded that although a smaller K_r can result in a good measurement for the threshold in the preamble field [4], it does not imply that a smaller K_r will always yield a better receiver performance when K is not zero.

F. Extinction Ratio Consideration for Burst-Mode Receiver

In the above analysis, we have evaluated the BER performance of the burst-mode receiver, but the system degradation due to the effect of accumulated CW optical power (or extinction ratio) from unmodulated optical sources in the optical network are not considered. In this section, we evaluate the BER degradation due to this finite extinction ratio.

The finite extinction ratio exists because in a bus or a star all-optical network, all transmitters have some residual CW optical power coupled into the fiber even when they are not transmitting. This effect is due to the inherent characteristics for the operation of optical transmitters in the network. Usu-

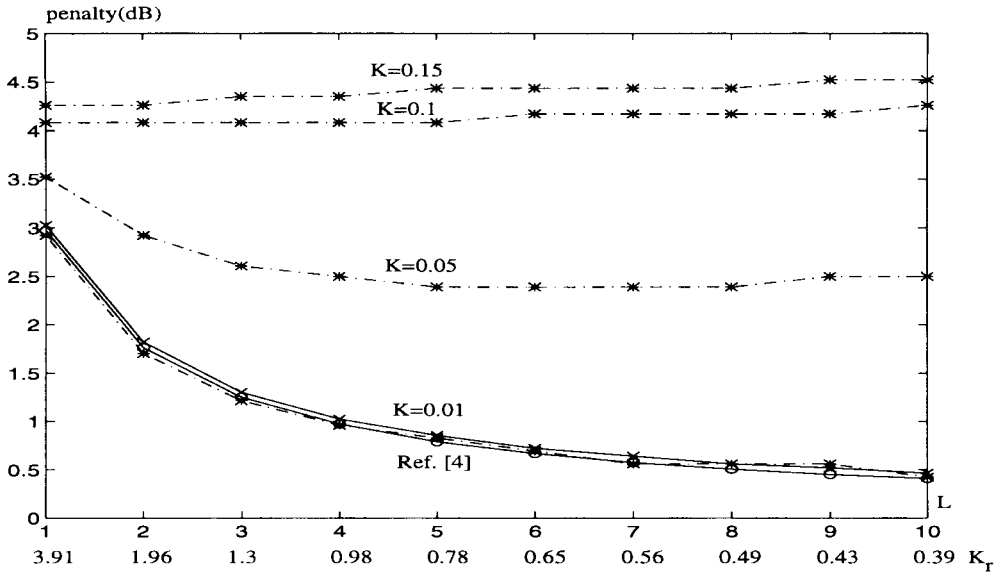

Fig. 9. SNR penalty of uncoded NRZ data versus K_r (or L-bits of preamble) for different K.

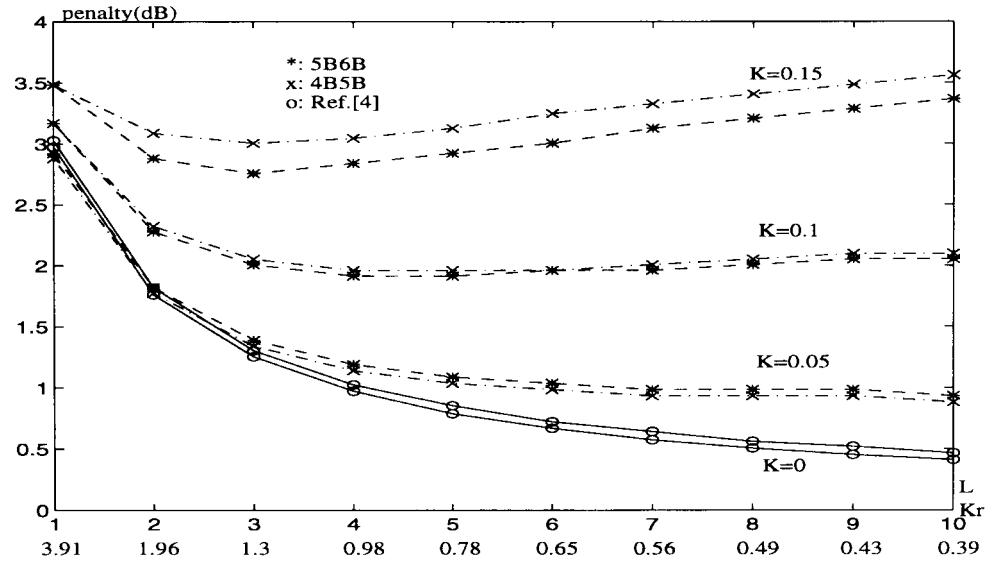

Fig. 10. SNR penalty of 4B5B/5B6B encoded data versus K_r (or L-bits of preamble) for different K.

ally, for an optical transmitter, in order to reduce the turn-on delay of the laser diode, the bias current for the optical source is set above the threshold. Therefore, a small but nonzero dc optical power is coupled into the optical fiber even when the transmitter is in the "off" state. For a dc-coupled burst-mode receiver, all these residual CW powers from different nodes will accumulate in the optical fiber which could seriously degrade the performance of the receiver. Consequently, more nodes in the network will degrade the extinction ratio more.

Form the definition of the extinction ratio $\gamma = P_{\text{off}}/P_{\text{on}}$, it is easily seen that the extinction ratio varies from packet to packet according to the amplitude of the input. In the worst case, when the input is at its minimum (which corresponds to the best receiver sensitivity), γ is at its maximum. In this case, the signal-to-noise ratio $Q[m, \gamma]$ for the receiver is

$$Q[m, \gamma] = Q \times \left[\frac{1+\gamma}{1-\gamma} \times \frac{e^{-(m-1)K} - e^{-mK}}{K} - \frac{2\gamma}{1-\gamma}\right]. \tag{16}$$

Here, we consider the effect of K to the receiver performance when extinction ratio exists. It should be noted that we only consider a worst case for the receiver, a good discussion about this problem can be found in [5], however, the effect due to K is ignored in [5].

In order to reduce the power penalty due to the extinction ratio, a good solution is proposed in [9]. By using a dark-level compensator subcircuit in the receiver, the circuitry can automatically measure and subtract out the signal due to the

TABLE III
THE CAPACITY PENALTIES OF THE NETWORK AND HOLDING TIME CONSTANT OF THE RECEIVER FOR UNCODED AND ENCODED SIGNALS

signal	coding penalty	capacity penalty	total	holding time
NRZ ($2^9 - 1$)	0%	18%	18%	20 ns
5B6B	16.6%	9%	25.6%	9 ns
4B5B	20%	8%	28%	8 ns

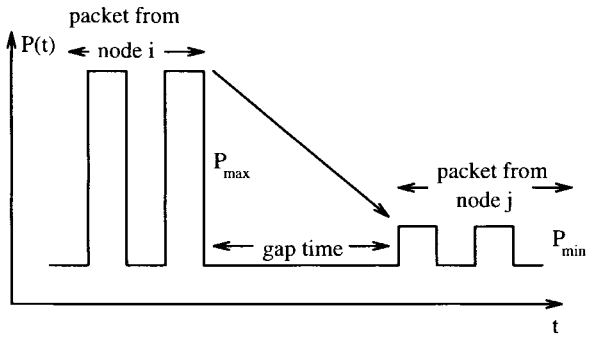

Fig. 11. The worst case for threshold shifting of a burst-mode receiver.

background light in the network, therefore, a good extinction ratio for the receiver can be achieved.

G. Network Capacity Penalty

In order to increase the network transmission efficiency, it is very desirable to reduce the gap time between two packets in the data bus. From the previous discussions, we realize that a small holding time constant of adaptive threshold control circuit can reduce the gap time but degrade the receivers BER performance. Therefore, there is a tradeoff between the time constant τ_f and network transmission efficiency.

Fig. 11 shows two packets transferred from node i and node j to node k. The worst case for the threshold shifting is when the first packet has the maximum received power and the second packet has the minimum, which requires the maximum discharge time for the adaptive threshold control circuit to reestablish the new threshold level. The maximum discharge time Δt_N is related to the maximum and minimum voltage amplitude $V_{th_{\max}}$ and $V_{th_{\min}}$ of the incoming data by

$$V_{th_{\min}} = V_{th_{\max}} \exp \frac{-\Delta t_N}{\tau_f}. \tag{17}$$

Thus, the gap time t_g between two packets should be

$$\begin{aligned} t_g &\geq \Delta t_N \\ &= \tau_f \cdot \ln \alpha_N \\ &= \frac{T}{K} \cdot \ln \alpha_N \end{aligned} \tag{18}$$

where T is the bit interval, K is the decay parameter of the receiver, and α_N is the dynamic range of the receiver. We define the channel utilization of the network as

$$\begin{aligned} \text{channel utilization} &= \frac{\text{packet length}}{\text{gap time + packet length}} \\ &= \frac{1}{1 + \dfrac{\ln \alpha_N}{K \cdot M}} \end{aligned} \tag{19}$$

where M is the number of bits in one packet and B is bit rate of the data link. Consequently, the capacity penalty β is defined as

$$\begin{aligned} \beta &= 1 - \text{channel utilization} \\ &= \frac{1}{1 + \dfrac{K \cdot M}{\ln \alpha_N}}. \end{aligned} \tag{20}$$

Here, we ignore the effect of rising time constant of the receiver, since the network capacity penalty due to the rising time is negligible comparing with the holding time. Equation (20) can be used to calculate the information transmission efficiency of the network. When the bit rate of the data link, packet length of the information and the dynamic range of the receiver are given, the capacity penalty is directly determined by the decay parameter K of the receiver.

As an example, let the bit rate of the network be 1 Gb/s and data pattern be uncoded ($N = 2^9 - 1$) or encoded (4B5B or 5B6B). Assume that the packet length is 53 bytes (ATM) and the dynamic range of receiver is 20 dB. Under the condition that the power penalty is $\leq$1 dB at a BER of 10^{-9}, the capacity penalties of the network and holding time constant of the receiver for uncoded and encoded signals are shown in Table III.

It is obviously that the above discussion is based on a natural discharge scheme for the threshold control circuit in the receiver. For fixed-sized packet transmission, by counting the number of bits in a packet [9], a "reset" signal can be used to accelerate the discharge time of the threshold control circuit. Hence, network transmission efficiency can be improved. However, by using this method, the burst-mode receiver will not be compatible with conventional receivers.

For variable-sized packets, the Frame-Start and Frame-End symbols which encapsulate the packet can be used to trigger the change of the decay parameter of the threshold control circuit. In order to do this, the data must be encoded by a line code (such as mBnB) to make sure that the Frame-Start and Frame-End symbols are unique. This encoding will lead to a capacity penalty automatically. Furthermore, there is increased complexity of the receiver. Thus, it may not be wise to employ such schemes after all.

H. Clock and Phase Recovery

For a multiaccess packet network, fast clock recovery or clock synchronization is a challenging problem due to the fact that short packet length is usually employed (e.g., ATM) and bursty packets may arrive with large phase variations. Up to now, several techniques of instantaneous clock synchronization for burst-mode data operation have been proposed. They are as follows:

1) global clock with correlator for phase detection [10];
2) quenched narrowband tank circuit [11];
3) gated-oscillators with PLL [12].

All these techniques have been experimentally demonstrated for fast clock recovery of burst-mode data. However, for method 1, the receiver requires a preamble field in the packet for the clock recovery and the recovered clock suffers a phase error. For method 2, there could be a frequency error. Thus, there is a power penalty associated with the clock recovery process for both methods. An analysis for the burst-mode clock recovery using these methods can be found in [10] and [13].

For method 3, instantaneous phase locking can be achieved without the use of any preamble. This is because every time the oscillator is started, the initial phase of the oscillation for each gated-oscillator in the circuitry is forced into phase synchronization with the input signal. However, the mechanism for the fast clock recovery is based on the transition of the input data sequence, thus, the jitter performance of the recovered clock is the same as that of the input data signal. Furthermore, the method requires a local oscillator oscillating at a frequency close to the input signal. The accuracy of this oscillator sets an upper limit on the maximum length of consecutive 1's or 0's present in the packet. Recently, new versions of this fast clock recovery device can eliminate the output jitter.

For the above techniques, method 3 is a very promising technique for the clock recovery of burst-mode data since it provides very fast clock and phase recovery (within one bit interval). In addition, the circuitry is simple which makes it suitable for high level circuit integration and for high-frequency operation.

Assume the technique of gated-oscillators with PLL is used in the clock recovery process, we can ignore the capacity penalty introduced since the clock and the phase can be recovered within one bit time.

I. Experimental Results for Burst-Mode Receivers

The BER measurement for burst-mode data is complicated by the gap time present among packets when a conventional BER measuring equipment is employed in the experiment. Since the BER tester cannot distinguish whether errors occurred in the packet or in the gap time, the BER measurements only indicates the average BER of the network. That is

$$\mathrm{BER}_c = ave(\mathrm{BER}_g + \mathrm{BER}_p) \tag{21}$$

where BER_g is the BER in the gap time, and BER_p is the BER in the packet.

Another difficulty for the BER measurement of burst-mode receiver is due to the reception of packets from multiple sources. Since the network protocol is based on multiaccess technique, the data received from different nodes are quite different from one another. In this case, a conventional BER test equipment can only read packets from a specific node where the BER tester's transmitter is located. It has also been suggested that the receiver's performance could be evaluated by measuring the closure of the eye diagram of the received packets in a multiaccess network [2].

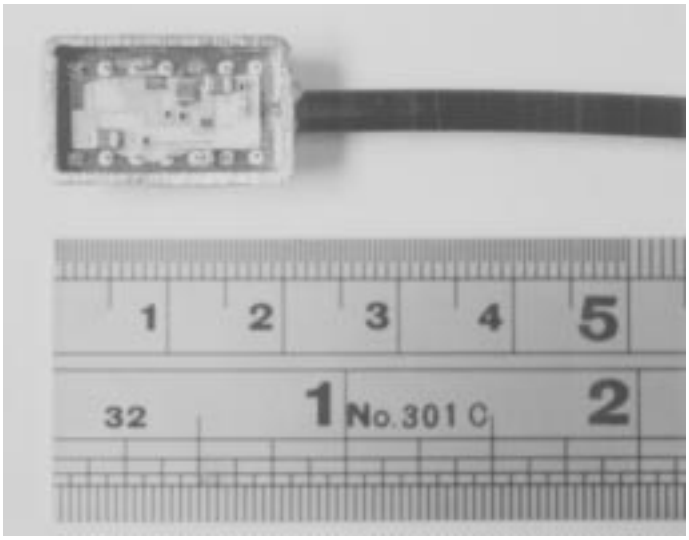

Fig. 12. Photograph of a packaged burst-mode receiver.

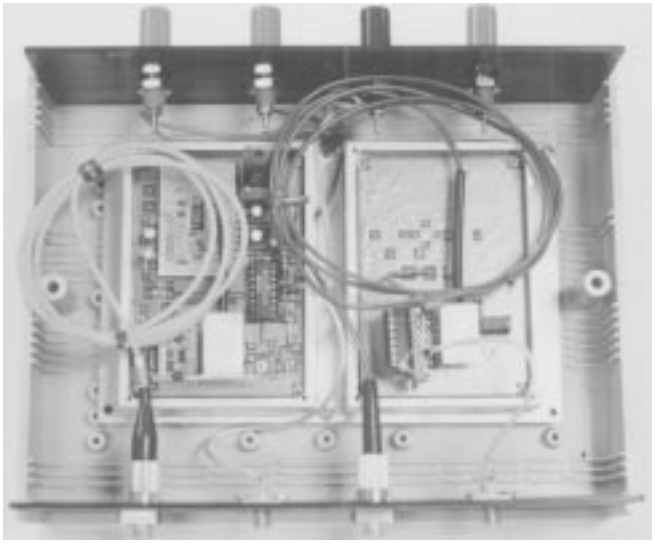

Fig. 13. Photograph of a burst-mode transceiver.

For the sake of facilitating the measurement of BER performance involving burst-mode receivers, we have derived an equation which relates the burst-mode BER to the continuous-mode BER. With the help of this equation, the burst-mode BER can be easily obtained.

Assuming a uniform gap time, the BER of the burst-mode receiver can be written as

$$P_{eb} \approx (1-\beta)P_{ec} + \frac{\beta}{n_g}\sum_{i=1}^{n_g}\frac{\exp\dfrac{-Q^2(i)}{2}}{\sqrt{2\pi}Q(i)} \tag{22}$$

where P_{ec} is the BER for the receiver when the input data is in continuous mode, $Q(i)$ is the Q-function of the ith bit in a consecutive string of 0's, and β is the capacity penalty of the network as defined in (20), which is approximated by

$$\beta \approx \frac{n_g}{n_g + M} \tag{23}$$

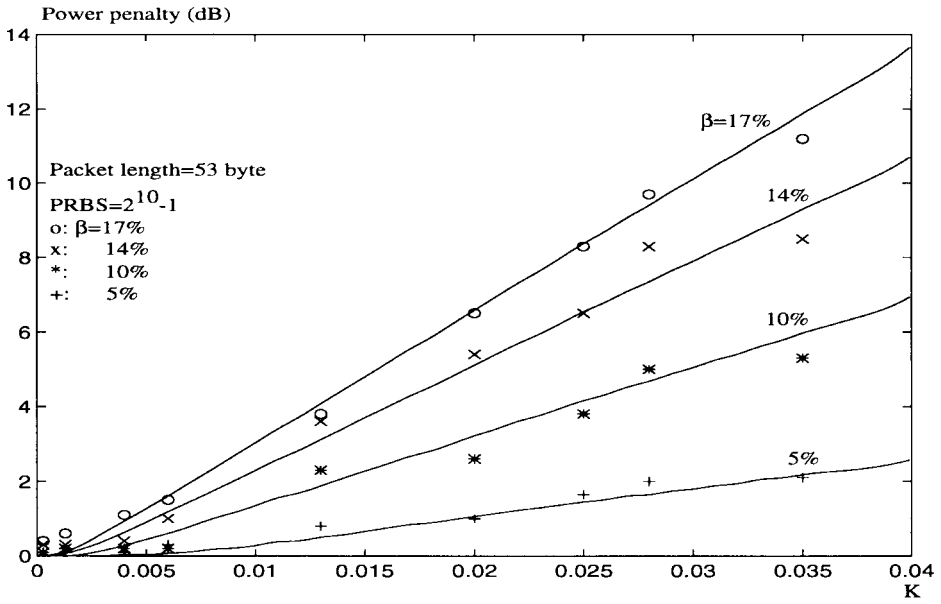

Fig. 14. Power penalty for a burst-mode receiver. $V_{\text{offset}} = 0$.

where n_g and M are the integer number of bits in the gap and packet, respectively.

We have verified this equation both theoretically and experimentally. For the experiment, the burst-mode receiver chip is obtained from AT&T Bell Laboratory [1], and is packaged at the Chinese University of Hong Kong. A photograph of the packaged burst-mode receiver is shown in Figs. 12 and 13. In Fig. 14 is shown the power penalty versus the decay parameter K for different capacity penalty at a BER of 10^{-9} with the voltage offset of the threshold set to zero. Here, the power penalty means the sensitivity penalty between the continuous mode and the burst-mode. The solid lines are computed from (22) and the discrete dots are the experiment results. The results agree very well with one another.

Therefore, to characterize the BER performance of the burst-mode communication, we can first measure the receiver's BER for continuous mode data, and then derive the receiver's BER for the burst-mode data by Fig. 14. For example, if the decay parameter K is 0.01 for a burst-mode receiver with a receiver sensitivity of -32 dBm for continuous mode reception, and assume the network capacity penalty is 10%, then from Fig. 14, we can derive the receiver's sensitivity to be about -31 dBm for burst-mode reception under the same bit rate.

J. Threshold Offset Consideration

For packet transmission in a network, if a natural discharge mechanism is employed in the adaptive threshold control circuit of the receiver, a threshold offset is needed. The reason is that, in burst-mode operation, there are silent intervals when no data is present. In these silent intervals, the threshold is not allowed to go to zero, otherwise random noise fluctuations will trigger the decision circuit and cause errors.

In order to prevent the threshold naturally discharging to zero level, a minimum dc offset should be set in the adaptive threshold detection circuitry. When the offset is increased, there is greater immunity to the random noise, but the receiver sensitivity will degrade and pulse width distortion will also result [1]. Therefore, it is necessary to search for an optimum offset level for the threshold to prevent noise interference occurring in the gap time among packets, while maintain a minimum power penalty caused by this offset.

We have investigated the power penalty of the receiver due to this offset both experimentally and analytically. The experimental and theoretical results are shown in Fig. 15. Fig. 15 is similar to Fig. 14, except that the offset of the threshold is set to be 1.2σ, where σ is the rms noise in the receiver. In the experiment, the bit rate of the data link is 100 Mb/s, the responsivity of the photo-detector is 0.94, the packet length is 53 bytes, the gap time length is generated by a programmable BER counter (HP71600B), and K is changed by replacing the capacitor in the adaptive threshold control circuit in the receiver. The receiver sensitivity is around -32 dBm for continuous mode.

The power penalty is 1 dB smaller for the case with an offset than that without an offset. This is because the measurement includes the BER occurred during the gap times. However, a large offset will result in pulse width distortion (PWD) which will also degrade the receiver performance.

When the threshold of the receiver is offsetted by V_{offset}, the sampling error τ in Fig. 16 can be estimated by

$$\tau \approx \frac{V_{\text{offset}}}{\dfrac{dV}{dt}} \approx \frac{t_r}{\dfrac{g(0)}{V_{\text{offset}}}} \tag{24}$$

where $t_r \approx 0.75/\text{BW}$, BW is the bandwidth of the receiver, and $g(0)$ is the peak voltage of the pulse. With a voltage offset, the Q-function must be modified by

$$Q = \begin{cases} \left(\dfrac{2g(\tau)}{g(0)} - 1\right)Q_c - \dfrac{V_{\text{offset}}}{\sigma} & \text{for bit 1} \\ Q(i) + \dfrac{V_{offset}}{\sigma} & \text{for } i\text{th bit 0} \end{cases} \tag{25}$$

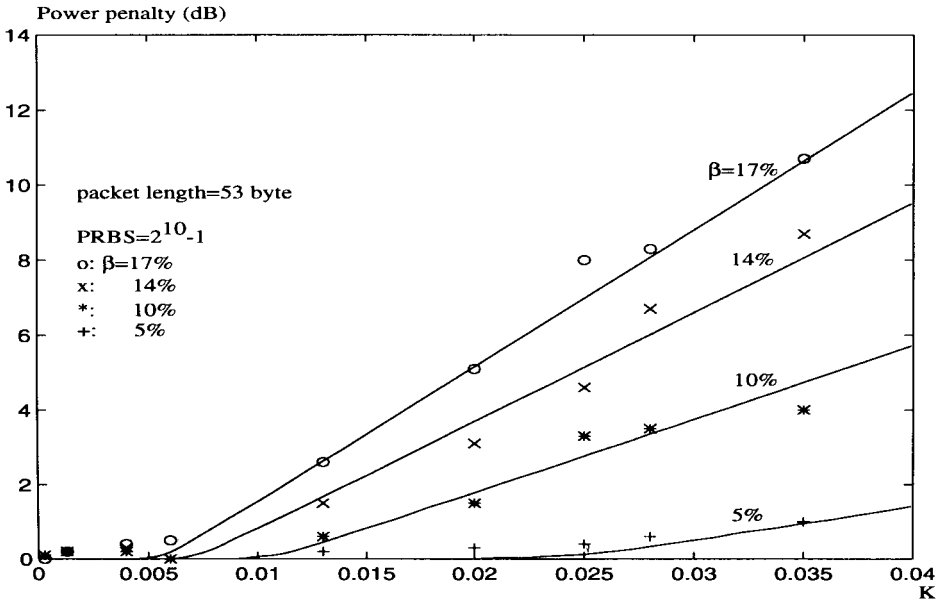

Fig. 15. Power penalty for a burst-mode receiver. $V_{\text{offset}} = 1.2\sigma$.

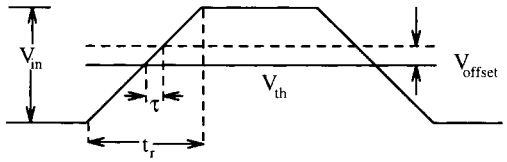

Fig. 16. The pulse width distortion and sampling error τ due to the threshold offset.

where $Q_c = (V_1 - V_0)/2\sigma$ is the conventional Q-function of the receiver, and $g(t)$ is the waveform of the pulse. By substituting (25) into (22), we can get the power penalty versus the offset for the normalized Gaussian and raised cosine waveform as shown in Fig. 17. It can be seen that the BER performance for Gaussian and raised cosine waveform are about the same. In addition, the power penalty (burst-mode relative to the continuous mode) can be reduced by increasing the offset but the inherent sensitivity of the receiver (continuous mode) will be degraded due to this offset.

III. Applications of Burst-Mode Receivers in Optical Multiaccess Networks

The architectures of all-optical multiaccess networks can be divided into three basic categories: bus/ring, tree and star topologies; and there are two signal transmission schemes, namely, regenerative and nonregenerative.

For regenerative transmission, the signals is regenerated by an optical transceiver. Due to the speed limitation of electronic processing in the repeaters (below 10 Gb/s), regenerative transmission is not suitable for ultra-high speed transmission.

Nonregenerative transmission is advantageous for all-optical networks due to the fact that it allows ultrahigh-speed transmission as well as making the network flexible, evolvable and reducing the network complexity. It is especially attractive with the availability of EDFA's. However, the network performance is constrained by physical problems such as fiber dispersion, accumulated amplifier noise and fiber nonlinearities. For the nonregenerative scheme, since the signal amplitudes and phases from different transmitters may vary from packet to packet, burst-mode receivers are needed.

In this section, we describe several novel applications for burst-mode receivers in optical communication networks as follows.

1) Supervisory system for long-hauled transmission systems using EDFA's. For long-hauled or undersea optical transmission systems using EDFA's as the repeaters, it is difficult to supervise and control these repeaters. We propose to use a nonregenerative all-optical multiaccess network to transmit supervisory signal for this undersea optical communication system using burst-mode receivers.
2) High-speed all-optical multiaccess network. Three types of broadband multiaccess network architecture are discussed. We point out that the burst-mode receiver is especially suitable for various all-optical multiaccess networks based on packet transmission.

A. Supervisory System for Long-Hauled Transmission Systems Using EDFA's

1) Techniques for the Supervisory Signal Transmission: For long-hauled transmission systems employing EDFA, especially for the undersea submarine systems, reliability is one of the most important issues. To guarantee the networks operating reliably, standby backup equipment and supervisory control are required. Whenever a fault is detected by the supervisory system, various parts of the transmission system may switch to their standby equipment. Usually, the supervisory (SV) signal should include information about the pumping laser diodes, line-signal level, fault locations, control signal, etc.

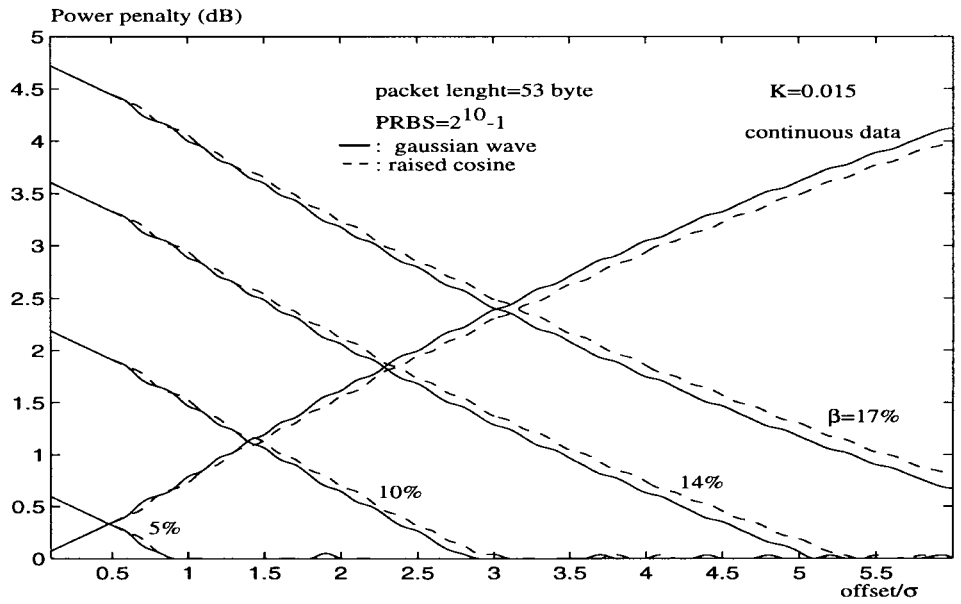

Fig. 17. Theoretical power penalty of the receiver due to the different threshold offset.

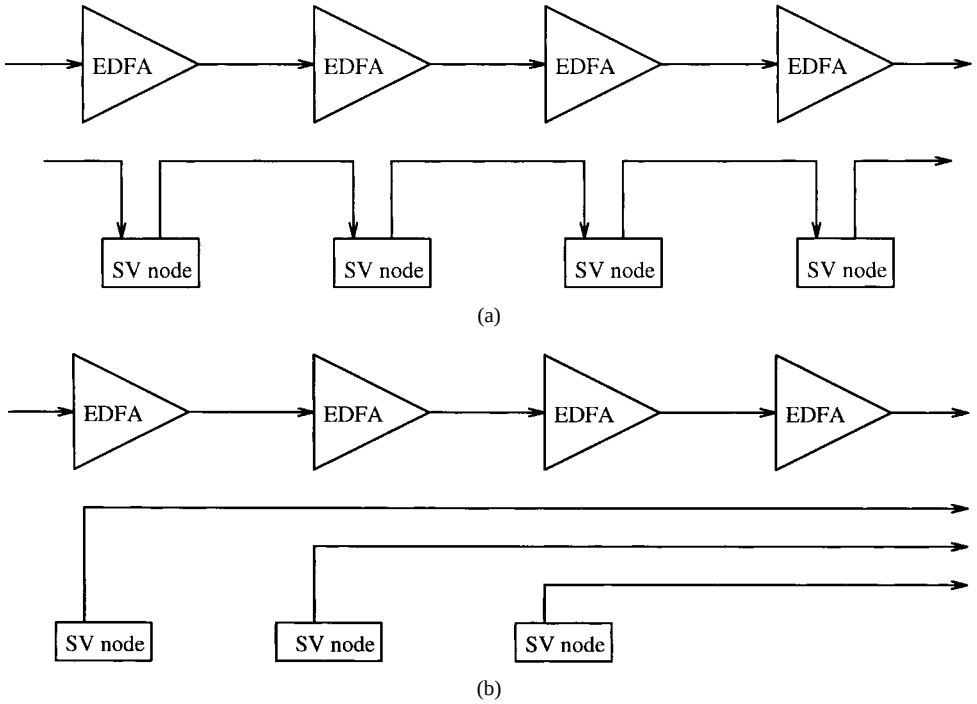

Fig. 18. Two schemes for the SV signal transmission in the system.

There are two potential techniques to transport the SV signal over the EDFA long-hauled systems [14] as follows:

1) termination and regeneration of SV signal at each EDFA repeater;
2) transparent channel through EDFA repeaters.

These two techniques are shown in Fig. 18. The first technique is the conventional method for carrying the SV signal. Each repeater first reads in the address of the received SV signal and reacts only when the address matches itself, otherwise it relays the signal to the next repeater. For the second technique, each repeater receives and sends its SV signal directly to the head-end independent of other repeaters. Essentially, the supervisory control at various repeaters formed a nonregenerative multiaccess network.

Up to now, several techniques have been proposed for transparent supervisory signal transmission in EDFA systems. They are as follows:

1) by modulating the pump laser diodes at each repeater node with a multi-Mb/s signal [14] or by modulating the spontaneous emission [15];
2) by using optical circulators to provide a reverse path for the amplified back-scattered OTDR [16] or for an amplified supervisory signal [17];
3) by using OTDR with pulse pump lasers [18].

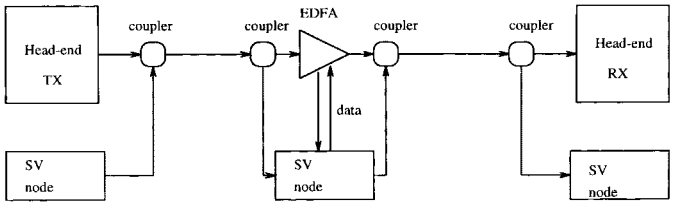

Fig. 19. Transmitting and regenerating scheme for SV signal transmission. Conventional repeaters are used in the supervisory node.

All the above techniques are sufficient for the system monitoring. However, it is impossible for the head-end to remote control the EDFA's in the system because each repeater can only write its message on the transparent channel but cannot read the information from the head-end terminals. In addition, only a small bandwidth SV control signal is provided by these techniques. Therefore, if N systems operate in parallel in N separate fibers, each system must provide its own SV channel.

Here, we propose two configurations for carrying broadband SV signals over EDFA systems. One belongs to the regenerative category and the other belongs to the transparent channel category. We shall describe and compare these two techniques below.

2) Termination and Regeneration of SV Signal at Each EDFA Repeater: A schematics for this technique is shown in Fig. 19. In the figure, the line signal (say, e.g., 2.5 Gb/s) is transmitted on one wavelength (1.55 μm) and is transparently passed through the chain of EDFA's, while the supervisory signal (say, e.g., 200 Mb/s) is transmitted on another wavelength (1.3 μm) using traditional optical transceiver (regenerative). Each EDFA repeater controller can read, write or relay the commands to and from the head-end controller via this SV channel.

If N systems operate in parallel in different fibers (to allow for redundancy and increase capacity), all the SV signals from different systems can be carried by this single SV channel. This technique is the conventional method for SV signal transmission. The power budget for the system is shown in Table IV.

3) Transparent Channel Through EDFA Repeaters: One of the problems of the above scheme is that if one of the repeaters for the SV channel fails, the entire supervisory signal will be broken. Therefore, the reliability for the SV system itself is severely degraded. To improve the reliability, it may be better to use a nonregenerative scheme for transmitting the SV channel.

The system configuration is shown in Fig. 20. Here the line signal (2.5 Gb/s) is still carried on one wavelength (1.55 μm) and the SV channel is on another wavelength (e.g., 1.56 μm), both within the EDFA gain region. The SV channel can be separated from the line signal with the help of a narrow-band filter. The system power budget is shown in Table V. In the above, FWD refers to the power budget for the forwarded transparent SV channel. The essential point is that the optical gain provided by each EDFA stage is sufficient to cover the attenuation within that section. RCV refers to the power budget for the SV channel from any node to

TABLE IV
POWER BUDGET FOR THE LINE CHANNEL AND REGENERATIVE SV CHANNEL IN EDFA SYSTEM

Parts	Line Channel	SV Channel
Bit Rate	2.5 Gb/s	200 Mb/s
Transmitter	0 dBm	0 dBm
Wavelength	1.55 μm	1.3 μm
Fiber Loss (40 km)	10 dB	20 dB
Splicing and Connector Loss	2 dB	2 dB
WDM Loss (2)	2 dB	2 dB
EDFA Gain	22 dB	NA
Receiver Sensitivity	NA	-38 dBm
Power Margin	8 dB	14 dB

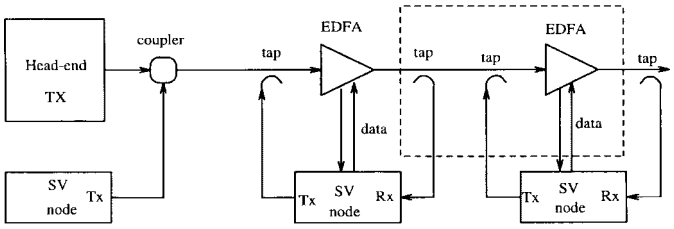

Fig. 20. Transparent scheme for SV signal transmission. Optical burst-mode receivers are used in the supervisory node.

any node (or to the head-end). It is also assumed that each EDFA stage can cover the attenuation within that section. With a proper arrangement of the burst-mode transmitters and receivers for the SV channel, there is a sufficient power budget left (29 dB) to protect against failure of one single EDFA stage.

In this application, TDMA packet transmission with a collision-free multi-access protocol and optical burst-mode receiver should be used in each supervisory node. Each node can read packets from any other node or send packets to the destinations if there is an available time slot. The operation of each node is independent of others. The main advantage of this method is that the reliability of the supervisory system is much improved compared with the regenerative scheme above. For example, even if one SV node fails, data packets from other SV nodes can still be transparently transmitted to the terminals or other nodes without any obstruction, and the failed node can be immediately located from the monitor at the head-end terminal. Failure of one EDFA stage is also protected.

B. Applications of Burst-Mode Receiver in High-Speed All-Optical Multiaccess Networks

In this section, the application of burst-mode receivers in broadband all-optical multiaccess packet networks is described. All-optical multiaccess network is a very active area of research (see, e.g., [19]). We shall describe the application of burst-mode receivers in star, bus and tree topologies, respectively.

1) Star Topology: For optical multiaccess network with star topology, many single-hop WDMA networks have been proposed, some with potential applications and some with full prototypes demonstrated. Some examples are Star-LAN [20], Fox/Hypass/Bhypass [21], Star-Track [22], Rainbow [23],

TABLE V
POWER BUDGET FOR THE LINE CHANNEL AND NONREGENERATIVE SV CHANNEL IN EDFA SYSTEM

Parts	Line Channel	SV Channel (FWD)	SV Channel (RCV)
Bit Rate	2.5 Gb/s	200 Mb/s	200 Mb/s
Transmitter	0 dBm	NA	−3 dBm
Wavelength	1.55 μm	1.56 μm	1.56 μm
Fiber Loss (40 km)	10 dB	10 dB	NA
Splicing and Connector Loss (2)	2 dB	2 dB	2 dB
Tap Loss (in)	1 dB	1 dB	10 dB
Tap Loss (out)	1 dB	1 dB	10 dB
Optical Filter	NA	NA	3 dB
EDFA Gain	22 dB	22 dB	22 dB
Receiver Sensitivity	NA	NA	−35 dBm
Power Margin	8 dB	8 dB	29 dB

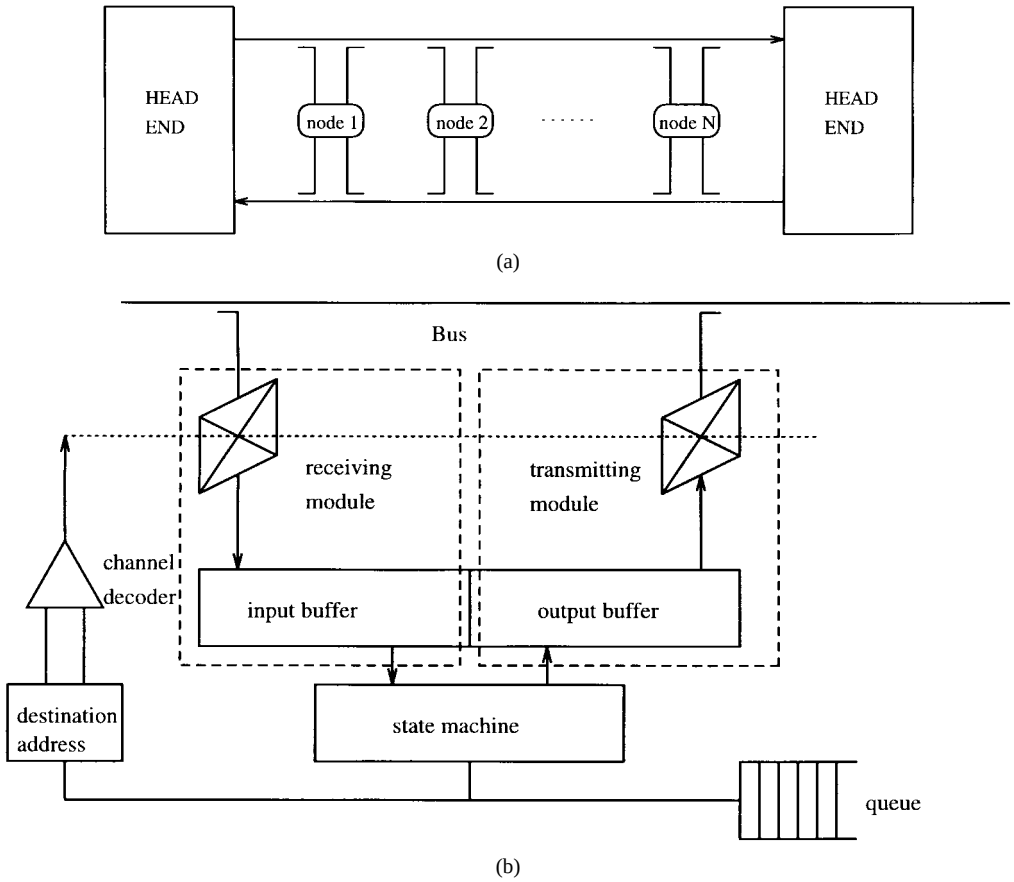

Fig. 21. The network topology and node structure for TCMA network.

WDMA [24], POPSMAC [25], etc. All these networks require tunable transmitters or tunable receivers or both. In order to support packet-switching, the tuning speed of the transmitters and receivers are assumed to be very fast in comparison with the packet length. Recently, there have been some encouraging advances in wavelength tunable transmitters and receivers that could support fast packet switching [26].

For these packet-switching networks, it is not possible to employ conventional receivers in the network, since they require long access time and are unable to process burst-mode packets from different nodes. Therefore, the development of burst-mode receivers is essential for these packet networks. In addition, burst-mode receivers can also support circuit-switching in these networks.

2) Bus Topology: For multiaccess networks with bus topology, many networks and protocols have been proposed. Some examples are: Fastnet [27], Expressnet [28], DQDB [29], ACTA [30], etc. In these networks, the headend simply sends empty time slots to the bus. For reception at a specific node, the receiver simply monitors the channel and reads in a slot when the packet's destination address matches its own address. For transmission, a node simply writes its packet to the bus at an available empty slot after the media access condition is satisfied. Of the above, ACTA is a very interesting protocol which is suitable for all-optical multiaccess implementation. This class of multi-channel networks is called tunable-channel multi-access networks (TCMA) (see Fig. 21, [31]).

In these bus topology all-optical networks, the packet transmission employs a nonregenerative scheme. Thus, the fiber attenuations and dispersions for different signal paths are quite different for various nodes. For signal reception, the receiver have to face the large variations both in amplitudes and phases for the received packets. Therefore, a burst-mode receiver has to be deployed.

3) Tree Topology: For multiaccess network with tree topology, a well-known example is the passive optical network (PON) using TDMA technology. There are many network proposals based on the tree architecture, such as TPON [32], MACNET [33], and APON [34], etc. Technologies for these applications have been developed quite well, and the network prototypes have been demonstrated or trailed in the field.

For most PON networks, the central office (CO) continuously sends its data to all the nodes via the passive optical splitters. Therefore, for the downlink, a conventional transmitter (at the CO) and a conventional receiver (at each node) can be used. However, for the uplink, packet collisions have to be avoided. The network thus allows only one node to transmit its packet to the CO at one time. Packets follow each other to the receiver at the CO are separated by a certain gap time.

It is obvious that in a tree topology all-optical TDMA network, a burst-mode receiver should be used in the CO. The receiver can effectively receive and handle bursty packets from various nodes with large geographical separation without severe synchronization requirement. In conclusion, burst-mode receivers are suitable for all these various types of all-optical multi-access packet networks.

IV. Conclusion

With the recent technological developments in high-speed ATM packet-switching and transmission, EDFA, WDM, TDMA, fast tunable optical devices, and multimedia applications, all-optical multiaccess packet networks have emerged as a feasible and promising candidate for the future ultra-high speed optical communications. These networks are very flexible, reliable, and scalable, and can have very high performance with simple topologies and protocols. One of the most important building blocks of these all-optical multiaccess networks is the burst-mode receivers. This newly developed receiver can instantaneously handle burst-mode data in the network. In this paper, we have proposed a complete theory to evaluate the receiver's performance, and the results of BER analysis is verified both theoretically and experimentally. This theory can provide a complete understanding of the BER performance of the burst-mode receivers.

We have also investigated the applications of burst-mode receivers in optical packet networks. We have proposed an application in the supervisory system of the EDFA transoceanic optical links. For high-speed all-optical multiaccess packet networks, we have discussed the role of burst-mode receivers in these networks with different topologies, thus showing that burst-mode receivers are very suitable for all these types of all-optical multiaccess packet networks.

References

[1] Y. Ota and R. G. Swartz, "Burst mode compatible optical receiver with large dynamic range," *J. Lightwave Technol.*, vol. 8, pp. 1897–1903, Dec. 1990.

[2] ———, "DC-1Gb/s burst mode compatible receiver for optical bus application," *J. Lightwave Technol.*, vol. 10, pp. 244–249, Feb. 1992.

[3] L. M. Lunardi, S. Chandrasekhar, R. G. Swartz, R. A. Hamm, and G. J. Qua, "High-speed burst-mode OEIC photoreceiver using InP/InGaAs heterojunction bipolar transistors," in *Proc. OFC'94*, San Jose, CA, 1994, paper TuH-2, pp. 30–31.

[4] C. A. Eldering, "Theoretical determination of sensitivity penalty of burst-mode fiber optic receiver," *J. Lightwave Technol.*, vol. 11, pp. 2145–2149, Dec. 1993.

[5] P. M. Valdes, "Performance of optical direct receivers using noise corrupted decision threshold," *J. Lightwave Technol.*, vol. 13, pp. 2202–2214, Nov. 1995.

[6] C. Su, L. K. Chen, and K. W. Cheung, "Inherent transmission capacity penalty of burst-mode receiver for optical multiaccess networks," *IEEE Photon. Technol. Lett.*, vol. 6, May 1994.

[7] Y. Ota *et al.*, "High-speed, burst-mode, packet-capable optical receiver and instaneous clock recovery for optical bus operation," *J. Lightwave Technol.*, vol. 12, Feb. 1994.

[8] G. Keiser, *Optical Fiber Communications*, 2nd ed. New York: McGraw-Hill, Inc., 1991.

[9] Y. Ota *et al.*, "Low-power, high-sensitivity 30 Mb/s burst-mode/packet receiver for PON application," in *Proc. OFC'94*, San Jose, CA, Feb. 1994, paper ThH-2, pp. 210–212.

[10] C. A. Eldering *et al.*, "Digital burst mode clock recovery technique for fiber-optic systems," *J. Lightwave Technol.*, vol. 12, Feb. 1994.

[11] Y. Nagasako *et al.*, "Fast timing extraction method for an optical passive bus," *Electron. Lett.*, vol. 26, no. 15, July 1990.

[12] M. Banu and A. E. Dunlop, "Clock recovery circuits with instantaneous locking," *Electron. Lett.*, vol. 28, no. 23, Nov. 1992.

[13] C. Su, L. K. Chen, and K. W. Cheung, "System degradation for clock and phase recovery of digital burst-mode receiver," in *Proc. ISCOM'93*, Taiwan, R.O.C., 1993.

[14] S. Matsuoka, Y. Yamabaysshi, K. Aida, and K. Nakagawa, "Supervisory signal transmission methods for optical amplifier repeater systems," in *IEEE Proc. GLOBECOM'90*, San Diego, CA, 1990, pp. 1846–1850.

[15] K. Shimizu, T. Mizuochi, and T. Kitayama, "Supervisory signal transmission experiments over 10,000 kM by modulated ASE of EDFA's," *Electron. Lett.*, vol. 29, no. 12, pp. 1081–1083, 1993.

[16] Y. Sato and K. Aoyama, "Optical time domain reflectometry in optical transmission lines containing in-line Er-doped fiber amplifiers," *J. Lightwave Technol.*, vol. 10, pp. 78–83, 1992.

[17] Y. Sato *et al.*, "Supervisory channel using fiber brillouin amplifiers for Er-doped fiber amplifier transmission systems," in *Tech. Dig., Opt. Amplifiers and Their Appl.*, 1992, paper ThA2.

[18] Y. W. Lai, Y. K. Chen, and W. I. Way, "Novel supervisory technique using wavelength-division-multiplexed OTDR in EDFA repeatered transmission systems," *IEEE Photon. Technol. Lett.*, vol. 6, Mar. 1994.

[19] Special Issue on "Broad-band optical networks," *J. Lightwave Technol.*, vol. 11, May/June 1993.

[20] I. M. I. Habbab *et al.*, "Protocols for very high-speed optical fiber local area network using a passive star topology," *J. Lightwave Technol.*, vol. 5, Dec. 1987.

[21] E. Arthurs *et al.*, "Multi-wavelength cross-connection for parallel processing computers," *Electron. Lett.*, vol. 24, no. 2, Jan. 1988.

[22] T. T. Lee *et al.*, "A broadband optical multicast switch," in *XIII Int. Switching Symp., ISS'90*, Sweden, May 1990.

[23] F. J. Janniello *et al.*, "A prototype circuit-switch multi-wavelength optical metropolitan-area network," *J. Lightwave Technol.*, vol. 11, May/June 1993.

[24] M. S. Chen *et al.*, "A media-access protocol for packet-switched wavelength division metropolitan area networks," *IEEE J. Select. Areas Commun.*, vol. 8, Aug. 1990.

[25] C. S. Li, M. S. Chen, and F. K. Tong, "POPSMAC: A media access protocol for packet-switched passive optical networks using WDMA," *J. Lightwave Technol.*, vol. 11, May/June 1993.

[26] F. K. Tong, "Recent developments in optical computer networks," in *IOOC'95*, Hong Kong, June 1995, paper ThC1-2.

[27] J. O. Limb *et al.*, "Description of fastnet—A unidirectional local-area communication network," *Bell Sys. Tech., J.*, vol. 61, 1982.

[28] F. A. Tobagi *et al.*, "Expressnet: A high performance integrated-service local area network," *IEEE J. Select. Areas Commun.*, vol. SAC-1, pp. 898–913, 1983.

[29] Standard IEEE802.6, "Distributed queue dual bus (DQDB) subnetwork of a metropolitan area network (MAN)," Dec. 1990.

[30] K. W. Cheung, "Adaptive-cycle tunable-access (ACTA) protocol: A simple high-performance protocol for tunable-channel multi-access (TCMA) networks," in *Proc. ICC'93*, Geneva, Switzerland, 1993, paper 16.1, pp. 166–171.
[31] K. W. Cheung, L. K. Chen, C. Su, C. T. Yeung, and P. T. To, "Tunable-channel multi-access (TCMA) networks: A new class of high-speed networks suitable for multimedia integrated networking," in *SPIE'93—Multigigabit Fiber Commun. Syst.*, San Diego, CA, July 1993.
[32] T. R. Rowbotham, "Local loop development in the UK," *IEEE Commun. Mag.*, June 1993.
[33] I. M. McGregor, "Implementation of a TDM optical network for subscriber loop applications," *J. Lightwave Technol.*, vol. 7, Nov. 1989.
[34] D. J. G. Mestdagh *et al.*, "ATM local access over passive optical networks," in *Proc. 3rd IEEE Workshop Local Opt. Networks*, Tokyo, Japan, Sept. 1991.

Chao Su was born in Wuhan, People's Republic of China (P.R.C.), on August 19, 1964. He received B.Eng. degree from Beijing University of Posts and Telecommunications, Beijing, in 1985, the M.Eng. degree from Wuhan Posts and Telecommunications Research Institute in 1988, and the Ph.D. degree from The Chinese University of Hong Kong in 1996.

From 1988 to 1992, he was a Technical Staff Member at Wuhan Posts and Telecommunications Research Institute, P.R.C. In 1996, he was a Postdoctoral Fellow in The Chinese University of Hong Kong. He is now with QPS Technology Inc., Canada. His research areas are in high-speed lightwave transmission system, optical network, fiber dispersion compensation, and optical receiver design.

Lian-Kuan Chen received the B.S. degree from National Taiwan University, Taiwan, in 1983, and the M.S. and Ph.D. degree from Columbia University, New York, NY, in 1987 and 1992 respectively.

For one and a half years, he was employed at General Instruments, USA. He joined the Chinese University of Hong Kong in 1992 and is currently an Associate Professor with the Department of Information Engineering. He was involved in various optical communications research in erbium-doped fiber amplifier distortion modeling, fiber lasers, and frequency planning for CATV systems. His current research interests are ultrahigh-speed all-optical networks, optical burst-mode receivers, network surveillance schemes, and photonic local access networks.

Kwok-Wai Cheung (SM'96) received the B.S. degree (First Honors) from the University of Hong Kong, in 1978, the M.S. degree from Yale University, New Haven, CT, in 1981, and the Ph.D. degree from Caltech, Pasadena, CA, in 1987.

In December 1992, he joined the Chinese University of Hong Kong and is currently a full Professor in the Department of Information Engineering. In January 1996, he was appointed the founding Director of the Information Networking Laboratories, a technology transfer organization for the Chinese University of Hong Kong. From 1987 to 1992, he was a Member of Technical Staff at Bell Communications Research, NJ. He has performed research in many areas, including lightwave system and device technology, high-speed network architectures and protocols, LAN/MAN and loop distribution networks, multimedia systems, and Internet/Web-based technologies. He has authored or coauthored about one hundred journal and conference publications, and holds five U.S. patents.

Dr. Cheung was awarded an Electronics Letters Premium in 1992. He is a member of OSA and SPIE.